## Cryo-STEM Mapping of Phase Transitions in Oxide Quantum Materials with Atomic Resolution

Noah Schnitzer, Lopa Bhatt, Ismail El Baggari, Berit H Goodge, David A Muller, Lena F Kourkoutis

DECTRIS

ARINA with NOVENA
Fast 4D STEM



DECTRIS NOVENA and CoM analysis of a magnetic sample.

Sample coursey: Dr. Christian Liebscher, May-Planck-Institut für Eisenforschung GmbH.

## Meeting-report



## Cryo-STEM Mapping of Phase Transitions in Oxide Quantum Materials with Atomic Resolution

Noah Schnitzer<sup>1</sup>, Lopa Bhatt<sup>2</sup>, Ismail El Baggari<sup>3,4</sup>, Berit H. Goodge<sup>2,5</sup>, David A. Muller<sup>2,6,\*</sup>, and Lena F. Kourkoutis<sup>2,6</sup>

Atomic-resolution scanning transmission electron microscopy (STEM) offers local, real-space measurements of material crystal structure, particularly in quantum materials where local inhomogeneities can confound ensemble characterization techniques. In many quantum materials the phases and properties of interest only emerge at low temperatures, making cryogenic characterization essential. Reduced mechanical stability under cryogenic conditions presents significant challenges for atomic-resolution STEM imaging and analysis, but advancements in technique have made routine sub-Å resolution imaging at liquid nitrogen temperatures possible, providing access to a wide range of exotic phases absent at ambient temperature [1, 2]. Beyond stabilizing low-temperature ground states, cryogenic temperature control is a powerful thermodynamic tuning knob for driving phase transitions. With conventional cryogenic sample holders, however, atomic-resolution STEM is limited to a single base temperature set by the cryogen, as actively heating above this point causes rapid boiling and accordant instability. Developments in MEMS-based cryogenic holders now allow local heating of the sample without significantly disturbing the thermal equilibrium of the cryogenic system, enabling atomic-resolution imaging at variable cryogenic temperatures, ranging to even above room temperature [3]. In addition, advances in high speed, high-dynamic-range electron counting detectors now provide sufficient performance for cryogenic 4D-STEM multislice ptychography datasets to be collected and reconstructed. Here, we apply this full range of cryo-STEM capabilities to structurally characterize phase transitions in strongly correlated oxide materials.

Ca<sub>2</sub>RuO<sub>4</sub> undergoes a metal-insulator transition in the bulk at 357 K, but epitaxial strain can alter this transition temperature as well as the nature of the phases on either side of the transition [4]. Under compressive strain, for example, as stabilized in an epitaxial thin film on LaAlO<sub>3</sub>, the metal-insulator transition is suppressed to ~230 K and generates a nanotextured phase coexistence below the transition temperature. Here, we leverage atomic-resolution cryo-STEM to both visualize the extent of the nanostructure over hundreds of nanometers and resolve the lattice structure of the component phases (Fig. 1a-b). Variable temperature measurements of the nanostructure provide insight into its origin in the competition between the elastic and electronic degrees of freedom governing the film (Fig. 1c).

Next, we study the double-perovskite manganite SmBaMn<sub>2</sub>O<sub>6</sub>, which undergoes a series of thermally driven electronic and magnetic phase transitions. Like Ca<sub>2</sub>RuO<sub>4</sub>, SmBaMn<sub>2</sub>O<sub>6</sub> also has a metal-insulator transition – here driven by charge order, which also is suggested to break symmetries to stabilize a putative low temperature polar phase [5,6]. Precisely tracking the position of the oxygen sites is critical to characterizing these broken symmetries and building a mechanistic understanding of these phase transitions, but conventional STEM imaging techniques (Fig. 2a) lack either the sensitivity or precision to do so in this complex heavily distorted system. Here, we demonstrate the capability of cryogenic multislice electron ptychography, achieved here with the 100 µs frame time of the EMPAD-G2 detector, to resolve the oxygen sublattice and thus fully characterize the coupling of the charge order to every site in the unit cell (Fig. 2b) [7-9].

<sup>&</sup>lt;sup>1</sup>Department of Materials Science and Engineering, Cornell University, Ithaca, NY, USA

<sup>&</sup>lt;sup>2</sup>School of Applied and Engineering Physics, Cornell University, Ithaca NY, USA

<sup>&</sup>lt;sup>3</sup>Department of Physics, Cornell University, Ithaca NY, USA

<sup>&</sup>lt;sup>4</sup>Rowland Institute at Harvard, Harvard University, Cambridge MA, USA

<sup>&</sup>lt;sup>5</sup>Max Planck Institute for Chemical Physics of Solids, Dresden, Germany

<sup>&</sup>lt;sup>6</sup>Kavli Institute at Cornell, Cornell University, Ithaca NY, USA

<sup>\*</sup>Corresponding author: david.a.muller@cornell.edu

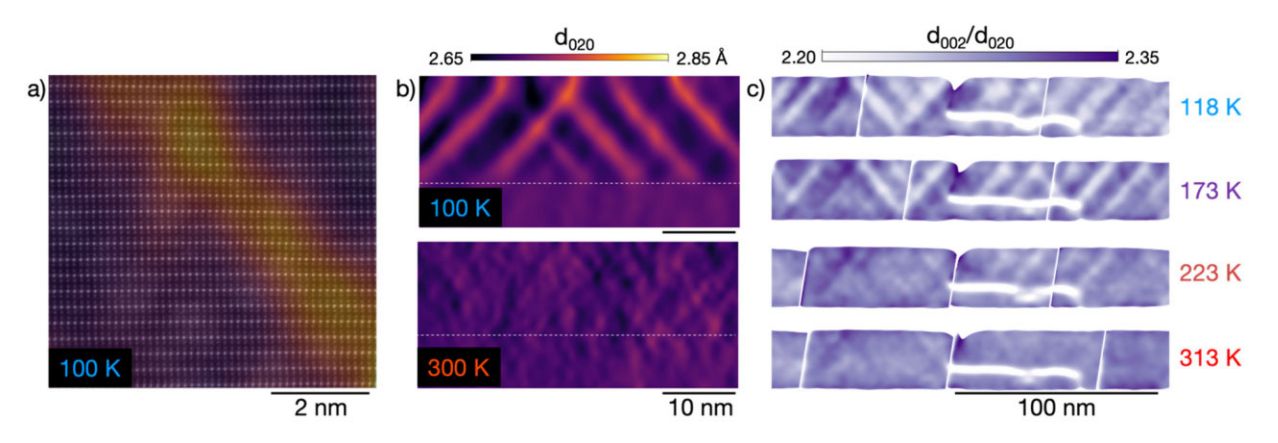


Fig. 1. Low temperature phase coexistence in  $Ca_2RuO_4$ . a) Atomic-resolution cryogenic STEM image overlaid with the in-plane (020) spacing, revealing a striped second phase. b) Larger field of view maps of the in-plane lattice spacing show a bifurcation at low temperatures absent in the fully strained film at room temperature. c) A series of maps of the ratio of the out-of-plane to in-plane lattice parameters extracted from montaged variable temperature cryo-STEM measurements visualize the dissolution of the nanostructure into the homogenous high temperature phase.

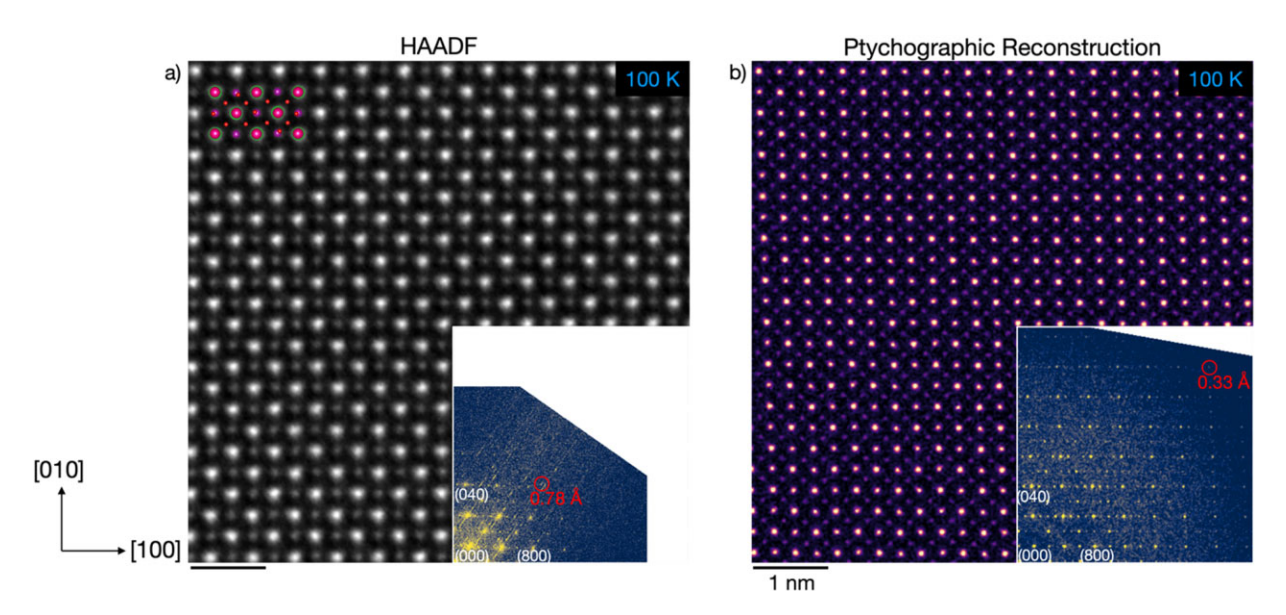


Fig. 2. Cryogenic multislice electron ptychography of a low temperature charge ordered phase in SmBaMn<sub>2</sub>O<sub>6</sub>. a) A high angle-annular dark field image acquired at  $\sim$ 100 K shows well resolved cation (Sm, Ba, Mn) sites but is insensitive to the light oxygen atomic columns. b) A multislice ptychographic reconstruction, also at  $\sim$ 100 K and cropped to show the same field of view as (a), reveals both the cation and oxygen sublattices with the high resolution and contrast needed for quantitative analysis. A small residual shear from sample drift is present in the reconstruction. Insets: Hann-windowed, log transformed FFTs indexed to the low temperature P2<sub>1</sub>am structure show the increased information limit of the ptychographic reconstruction.

## References

- 1. BH Savitzky et al., Ultramicroscopy 191 (2018), p. 56. doi:10.1016/j.ultramic.2018.04.008
- 2. I El Baggari et al., PNAS 115(7) (2018), p. 1445. doi:10.1073/pnas.1714901115
- 3. BH Goodge et al., Microsc. and Microan. 26(3) (2020), p. 439. doi:10.1017/S1431927620001427
- 4. M Braden et al., Physical Review B 58(2) (1998), p. 847. doi:10.1103/PhysRevB.58.847
- 5. D Morikawa et al., J. Phys. Soc. Jpn. 81 (2012), p. 093602. doi:10.1143/JPSJ.81.093602
- 6. H Sagayama et al., Phys. Rev. B 90 (2014), p. 241113. doi: 10.1103/PhysRevB.90.241113
- 7. Z Chen et al., Science 372(6544) (2021), p. 826. doi:10.1126/science.abg2533
- 8. H Philipp et al., Microsc. and Microan. 28(2) (2022), p. 425. doi: 10.1017/S1431927622000174
- 9. This work was supported by the National Science Foundation (Platform for the Accelerated Realization, Analysis, and Discovery of Interface Materials (PARADIM)) under Cooperative Agreement No. DMR-2039380 and by the U.S. Department of Energy, Office of Science, Office of Basic Energy Sciences, under Contract No. DE-SC0019414. The authors acknowledge the use of facilities and instrumentation supported by NSF through the Cornell University Materials Research Science and Engineering Center DMR-1719875, a Helios FIB supported by NSF (DMR-1539918), and FEI Titan Themis 300 acquired through NSF-MRI-1429155, with additional support from Cornell University, the Weill Institute and the Kavli Institute at Cornell. We thank Yorick A. Birkholzer, Hari Nair, Darrell G. Schlom, Anna S. Park, Evan Krysko, Jacob Steele, Shigeki Yamada, Taka-hisa Arima, Alemayehu S. Admasu, Jaewook Kim, and Sang-Wook Cheong for providing samples and Oleg Y. Gorobtsov, Ziming Shao, Jacob Ruf, Kyle M. Shen, and Andrej Singer for X-ray characterization.